RESEARCH ARTICLE

# Genome-wide identification and annotation of HIF-1α binding sites in two cell lines using massively parallel sequencing

Kousuke Tanimoto · Katsuya Tsuchihara ·
Akinori Kanai · Takako Arauchi · Hiroyasu Esumi ·
Yutaka Suzuki · Sumio Sugano

**Abstract** We identified 531 and 616 putative HIF-1α target sites by ChIP-Seq in the cancerous cell line DLD-1 and the non-cancerous cell line TIG-3, respectively. We also examined the positions and expression levels of transcriptional start sites (TSSs) in these cell lines using our TSS-Seq method. We observed that 121 and 48 genes in DLD-1 and TIG-3 cells, respectively, had HIF-1α binding sites in proximal regions of the previously reported TSSs that were up-regulated at the transcriptional level. In addition, 193 and 123 of the HIF-1α target sites, respectively, were located in proximal regions of previously uncharacterized TSSs, namely, TSSs of putative alternative promoters of protein-coding genes or promoters of putative non-protein-coding transcripts. The hypoxic response of DLD-1 cells was more significant than that of TIG-3 cells with respect to both the number of target sites and the degree of induced changes in transcript expression. The Nucleosome-Seq and ChIP-Seq analyses of histone modifications revealed that the chromatin formed an open structure in regions surrounding the HIF-1α binding sites, but this event occurred prior to the actual binding of HIF-1α. Different cellular histories may be encoded by chromatin structures and determine the activation of specific genes in response to hypoxic shock.

**Keywords** HIF-1 alpha · Hypoxia · ChIP-Seq · Transcriptome

K. Tanimoto · A. Kanai · T. Arauchi · Y. Suzuki (✉) ·
S. Sugano
Graduate School of Frontier Sciences, The University of Tokyo,
5-1-5 Kashiwanoha, Kashiwa, Chiba 277-8562, Japan
e-mail: ysuzuki@k.u-tokyo.ac.jp

K. Tsuchihara · H. Esumi
Cancer Physiology Project, Research Center for Innovative
Oncology, National Cancer Center Hospital East, 6-5-1
Kashiwanoha, Kashiwa, Chiba 277-8577, Japan

## Introduction

Cancer cells in solid tumors are frequently exposed to limited oxygen environments because aberrantly growing cancer cells can cause a shortage of blood flow (Pouyssegur et al. 2006; Harris 2002; Keith and Simon 2007). Hypoxia is a term that is used to describe such cellular environments, which have an oxygen concentration between 0.02 and 3% (Thomas and Johannes 2007). It is important to understand the behavior of cancer cells under hypoxia because hypoxic conditions can be utilized to develop a therapeutic method to treat cancers (Fyles et al. 1998; Nordsmark et al. 1996). If cancer cells were vulnerable to hypoxia, they would lose their ability to survive. In addition, controlling the hypoxic responses of cells may lead to new clinical therapeutics not only for solid tumors (Semenza 2003; Semenza 2010) but also for tissue ischemia and several inflammatory diseases (Fraisl et al. 2009; Semenza 2000).

Tumor cells adapt to hypoxic conditions through modifications of their gene expression patterns. For example, ATP metabolism changes from oxidative phosphorylation to anaerobic glycolysis. During this process, glucose uptake is enhanced, angiogenesis is induced to obtain a sufficient blood supply, and cell migration is promoted (Harris 2002; Pouyssegur et al. 2006; Gatenby and Gillies 2004; Hirota and Semenza 2006; Keith and Simon 2007). The central regulators of these changes in gene expression, which collectively lead to changes in cellular responses,

are the transcription factors hypoxia-inducible factors 1 and 2 (HIF-1/2) (Wang and Semenza 1995; Tian et al. 1997). Both HIF-1 and HIF-2 consist of two subunits, HIF-α and HIF-β (or ARNT). The α-subunit (HIF-1α, HIF-2α) is the oxygen-sensitive subunit. Under hypoxic conditions, HIF-1α (or HIF-2α) translocates from the cytoplasm to the nucleus and dimerizes with HIF-β. The HIF heterodimer complex binds to a sequence motif called the hypoxia response element (HRE) and activates the expression of genes that are necessary for cellular survival under hypoxic conditions (Maxwell 2005; Poon et al. 2009). Although HIF-1α demonstrates extensive sequence similarity to HIF-2α and is regulated via the same mechanism, HIF-1 and HIF-2 are assumed to possess distinct biological roles. HIF-2α expression is restricted to particular cell types, whereas HIF-1α is expressed ubiquitously (Wiesener et al. 2003). Additionally, genes encoding glycolytic enzymes such as PGK1 and GLUT1 are unique targets of HIF-1 (Wenger et al. 2005; Raval et al. 2005).

Because of the inferred important roles of HIF-1α, there have been several attempts to comprehensively identify HIF-1α targets (Ortiz-Barahona et al. 2010). Although computational methods alone may still require further innovation due to the ambiguity of the HRE motif, the combination of computational methods and expression analyses using microarrays has proven to be a powerful approach (Benita et al. 2009). More recently, several papers have reported the identification of HIF-1α binding sites based on chromatin immunoprecipitation and microarray (ChIP-chip) technology (Mole et al. 2009; Xia et al. 2009; Xia and Kung 2009). These studies have reported that about 400–500 of the HIF-1α binding sites in the human genome and approximately 70% of the HIF-1α binding sequences contain HREs.

Recent microarray-based approaches have produced far more information regarding HIF-1 targets than have conventional methods. However, these microarray methods have several limitations; namely, they cannot be used to analyze previously uncharacterized genes, for example, intergenic transcripts or transcripts of alternative promoters (Davuluri et al. 2008; Landry et al. 2003). In addition, the resolution of the data does not exceed the intervals of the DNA probes. The recently developed massively parallel sequencing technologies have provided a potential means to improve upon these methods. For example, the Illumina GA sequencer can sequence 200–250 million sequences per run. By utilizing Illumina GA and ChIP technologies (ChIP-Seq), the binding sites of several transcription factors have been reported (Valouev et al. 2008; Robertson et al. 2007; Kwon et al. 2009; Welboren et al. 2009; Park 2009). On the other hand, we also developed a method for sequencing the 5′-ends of mRNAs by combining our oligo-capping technique with the Illumina GA sequencer

(Tsuchihara et al. 2009). This method, which we named TSS-Seq, enables us to obtain precise information regarding the positions of the transcriptional start sites (TSSs) together with their expression levels in a high-throughput manner. In our previous report, we applied TSS-seq to observe gene expression changes in response to hypoxia in several cell lines (Tsuchihara et al. 2009).

To identify TSSs with hypoxic responses elicited directly by HIF-1α binding, we performed HIF-1α ChIP analysis and combined the resultant data with the TSS-Seq data. Furthermore, we carried out Illumina GA sequencing analysis using micrococcal nuclease-digested genomic DNA (Nucleosome-Seq) (Albert et al. 2007; Jiang and Pugh 2009; Schones et al. 2008). We examined the changes in nucleosome structure caused by HIF-1α binding and the subsequent transcriptional activation. We also examined the chromatin statuses surrounding the HIF-1α binding sites by ChIP-Seq analysis of RNA polymerase II (pol II) and a series of histone modifications, namely, H3K4 trimethylation (H3K4me3), H3 acetylation (H3Ac) and H3K27 trimethylation (H3K27me3) (Barski et al. 2007). H3K4me3 and H3Ac are known to be characteristic of an open chromatin structure, and H3K27me3 is characteristic of a closed chromatin structure. A colorectal cancer epithelial cell line (DLD-1) and a normal embryonic lung fibroblast cell line (TIG-3) were used for these analyses. Here, we report the genome-wide identification and characterization of HIF-1 targets using several types of massively parallel sequencing analyses. We further compared the observed targets between DLD-1 cells and TIG-3 cells to examine the cellular responses characteristic of these cells.

## Materials and methods

### Accession numbers

The short-read tag sequences used in the present work have been deposited in DDBJ under the following accession numbers: SRA003625 (TSS-Seq data), DRA000007-000008 and DRA000190-000191 (pol II ChIP-Seq data), DRA000073-000075 and DRA000003 (Nucleosome-Seq data), DRA000178-000185 (HIF-1α ChIP-Seq data), DRA000277-000284 (H3K4me3 ChIP-Seq data), DRA000285-000288 and DRA000293-000296 (H3Ac ChIP-Seq data) and DRA000289-000292 and DRA000297-000300 (H3K27me3 ChIP-Seq data).

The data generated in this study are accessible via following URL in BED file format: http://www.dbtss.hgc.jp/cgi-bin/downloader2.cgi/chip.tar.gz (ChIP-Seq data), http://www.dbtss.hgc.jp/cgi-bin/downloader2.cgi/nucleosome_bed.tar.gz (Nucleosome-Seq data), http://www.dbtss.hgc.jp/

cgi-bin/downloader2.cgi/rnaseq.tar.gz (RNA-Seq data) and
ftp://ftp.hgc.jp/pub/hgc/db/dbtss/dbtss_ver7/bed_files/ (TSS-Seq data).

Cell culture

The human colorectal cancer cell line DLD-1 (Japan
Health Science Research Resources Bank cell number
JCRB9094) was maintained in Dulbecco's Modified
Eagle's Medium (DMEM, Nissui) Supplemented with 10%
fetal calf serum, 4.5 g/l glucose, and antibiotics. The
human normal embryonic lung fibroblast cell line TIG-3
(Japan Health Science Research Resources Bank cell
number JCRB0506) was maintained in MEM (GIBCO)
Supplemented with 10% fetal calf serum and antibiotics.
The cells were cultured under standard conditions and
subjected to hypoxic shock (1% $O_2$) in a similar manner.

Construction of the ChIP-seq library and analysis
of ChIP-seq tags

DLD-1 and TIG-3 cells ($1 \times 10^8$) were fixed using a final
concentration of 1% formaldehyde at room temperature for
10 min. To quench the reaction, 150 mM (final concentration) glycine was added to the samples followed by a
5-min incubation. The cells were washed twice with PBS,
harvested and then lysed in 5 ml of Lysis Buffer 1 (50 mM
HEPES–KOH, pH 7.5, 140 mM NaCl, 1 mM EDTA, 10%
glycerol, 0.5% NP-40, 0.25% Triton X-100). The lysates
were incubated at 4°C for 10 min and centrifuged at
1,500 rpm for 5 min at 4°C. The pellets were then resuspended in 5 ml of Lysis Buffer 2 (10 mM Tris–HCl, pH
8.0, 200 mM NaCl, 1 mM EDTA, 0.5 mM EGTA), incubated at room temperature for 10 min, and centrifuged at
1,500 rpm for 5 min at 4°C. The pellets were resuspended
in 1 ml of Lysis Buffer 3 (10 mM Tris–HCl, pH 8.0,
100 mM NaCl, 1 mM EDTA, 0.5 mM EGTA, 0.1%
Na-deoxycholate, 0.5% N-lauroylsarcosine) and sonicated
with 18 cycles of 30 s each on ice using a sonicator
(TOMY SEIKO). One hundred microliters of 10% Triton-
X 100 was added to the samples, and the cell lysates were
centrifuged for 10 min. Fifty microliters of the supernatant
was saved for the controls (named whole cell extract
(WCE) DNA). Washed magnetic beads bound to 10 μg of
rabbit polyclonal anti-HIF-1α antibody (Novus Biologicals,
Inc., NB100-134), monoclonal anti-RNA polymerase II
antibody (Abcam, ab817), monoclonal anti-H3K4me3
antibody (ab1012), polyclonal anti-H3Ac antibody (Millipore, 06-599) or monoclonal anti-H3K27me3 antibody
(ab6002) was added to the supernatant. The samples were
rotated at 4°C overnight and washed 8 times with 1 ml of
wash buffer (50 mM HEPES–KOH, pH 7.5, 500 mM LiCl,
1 mM EDTA, 1% NP-40, 0.7% Na-deoxycholate) and once

with TE buffer containing 50 mM NaCl. The sample was
then eluted with 200 μl of elution buffer (1 M Tris–HCl,
pH 8.0, 0.5 M EDTA, pH 8.0, 1% SDS) at 65°C for
15 min. The supernatant was transferred to a new tube and
incubated at 65°C overnight. Concurrently, 150 μl of elution buffer was added to the saved WCE-DNA, and the
samples were incubated at 65°C overnight. Next, 200 μl of
TE and 8 μl of 10 mg/ml RNase A (Funakosi) were added
to the IP and WCE DNA samples. The samples were then
incubated at 37°C for 2 h. Subsequently, 4 μl of 20 mg/ml
proteinase K (Takara) was added to the samples, which
were then incubated at 55°C for 2 h. The DNA samples
were purified using TRIzol LS (Invitrogen) and ethanol
precipitation. Samples destined for ChIP-seq by Illumina
GA were prepared according to the manufacturer's
instructions.

Computational procedures

The generated ChIP-Seq tags were mapped to the reference
human genome sequences (hg18), and the tags that were
uniquely mapped allowing two-base mismatches were
used. The binding sites of HIF-1α, RNA polymerase II and
histone modifications, based on the short-read tag information, were identified as follows: the regions encompassed by the mapped tag sequences were extended to
120 bp, which reflected the insertion sites of the sample
DNA fragments. For each genomic position, the number of
overlapping extended tags was counted. Based on the
calculated tag information, the sum of the included tags
was evaluated to determine whether more than a tenfold
difference between the immunoprecipitation (IP) and the
whole cell extract (WCE) was present. Genomic regions in
which positive enrichment of the tags continued for more
than 121 bp were then selected. Among these regions,
those containing more than 5 different sequence tags were
identified as potential HIF-1α and RNA polymerase II
binding sites. We normalized the tag counts for each region
to tags per million (ppm) and divided the results by the
length of the region (ppm/bp). These values were determined as the peak strength in this study. In the HIF-1α
ChIP-Seq analysis, if the identified regions demonstrated
an overlap between 1% $O_2$ (hypoxia) and 21% $O_2$
(normoxia), regions with more than a twofold (hypoxia/
normoxia) change in peak strength were identified as
"bindings enriched in hypoxia." The statistical significance
determined for this selection procedure compared to
the background rate was evaluated using Poisson probabilities as previously described (Robertson et al.
2007):$P(x, \lambda) = 1 - \sum_{t=0}^{x} \frac{e^{-\lambda}\lambda^t}{t!}$,where $P(x,\lambda)$ is the probability
of enrichment, $\lambda$ is the expected tag number in the 121-bp

window calculated for the WCE sample, and $x$ is the observed tag number in the 121-bp window.

To analyze the gene expression changes in the transcription factors in DLD-1 and TIG-3 cells, 140 transcription factors were selected in TRANSFAC (Rel. 2010.1). The consensus sequences of the transcription factors were also evaluated using MATCH with cutoff values determined using minFP, which minimizes false-positive results. The enrichment of the detected putative binding sites in the HIF-1α target genes in DLD-1 cells, TIG-3 cells and both cell lines were evaluated by calculating the hypergeometric distributions. Putative transcription factor binding sites that were statistically significantly enriched ($P < 0.05$) in the respective groups were selected. For details, see Supplementary Table 3.

### TSS-Seq analysis and RNA-Seq analysis of polysome fractions

TSS-Seq tags were prepared and analyzed as described in the reference (Tsuchihara et al. 2009). After clustering the TSS-tags using 500-bp bins, representative TSSs were selected as the position from which the largest number of TSS tags was mapped. The selected representative TSSs were used for further analyses.

For the RNA-Seq analysis of polysome-incorporated RNA, the cytoplasmic fraction was isolated from DLD-1 cells using the PARIS Kit (Ambion, AM1921). Polysome-incorporated fractions were further fractionated from cytoplasmic fraction using the sucrose-density-gradient method described in the reference (Koritzinsky and Wouters 2007). Thirty-six-base-pair single-end-read RNA-Seq tags were generated using an Illumina GA sequencer according to the standard protocol. RNA-Seq tags that were mapped to the human reference genome sequences without any mismatches were used. RNA-Seq tags corresponded to RefSeq transcripts when their genomic coordinates overlapped. Details of the characterization and the RNA-Seq libraries are presented in Supplementary Fig. 6.

### Construction of the nucleosome-Seq library and analysis of nucleosome tags

Cells were cultured to 80% confluence and treated with micrococcal nuclease to generate mononucleosomes using the ChIP-IT Express Enzymatic Kit (active motif). The cells were formaldehyde-cross-linked prior to the nucleosome isolation. Cross-linking was performed with fixation solution (DMEM, 1% formaldehyde) for 10 min at room temperature. The cells were then washed with PBS, and the cross-linking reaction was stopped by incubating the cells with a glycine quenching solution (PBS glycine buffer) for 5 min at room temperature. After the dishes were washed

with PBS, an ice-cold cell scraping solution was added. The cells were then harvested and resuspended in ice-cold lysis buffer, incubated on ice for 30 min, and homogenized by 15–20 strokes with a Dounce homogenizer. The nuclei were suspended in digestion buffer and pre-warmed in this solution for 5 min at 37°C. An enzymatic cocktail (200 U/ml) was added to the sample, and the digestion reaction was incubated at 37°C for 15 min. After the reaction was stopped with EDTA, the nuclei were pelleted by centrifugation, and the supernatants were collected. Formaldehyde cross-linking was reversed by the addition of 5 M NaCl and RNase followed by an incubation at 65°C for more than 4 h. Proteinase K was added to the samples, and the mixtures were incubated at 42°C for 1.5 h. DNA was purified by phenol/chloroform extraction and ethanol precipitation. The extracted DNA was used for the sample preparation for Illumina GA according to the manufacturer's instructions.

### Real-time PCR analysis

Real-time PCR primers were designed within the identified HIF-1α binding sites. Primer3 (http://www.frodo.wi.mit.edu/primer3/) was used to design the primers. The fold enrichment at each locus was calculated according to the ΔΔCt method. The primer sequences are presented in Supplementary Table 1.
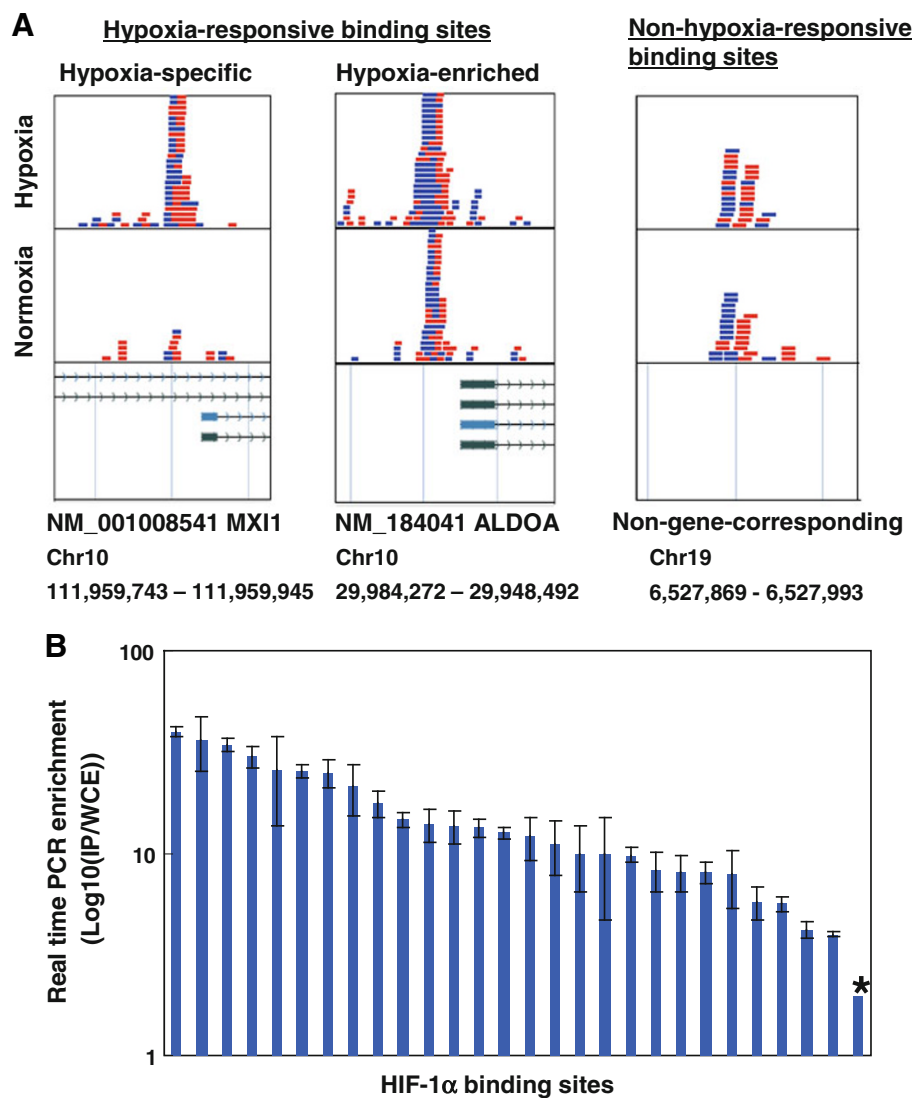
## Results and discussion

### Identification of HIF-1α binding sites

Using 22,315,752 and 15,389,864 36-bp single-end-read sequence tags generated for the ChIP-Seq analysis of DLD-1 and TIG-3 cells (Supplementary Fig. 1), we searched for HIF-1α binding sites by quantifying the local enrichment of tags (Robertson et al. 2007) (see "Materials and methods"). Next, we classified the putatively identified binding sites as "hypoxia-responsive" or "non-hypoxia-responsive." "Hypoxia-responsive" binding sites were the regions identified only under hypoxia or the regions in which the associated ChIP-Seq tags were enriched more than twofold under hypoxia. "Non-hypoxia-responsive" binding sites were those that did not show more than a twofold change in tag concentrations between normoxia and hypoxia. A typical example for each category is shown in Fig. 1a. As summarized in Table 1, there were 531 and 616 "hypoxia-responsive" HIF-1α binding sites in DLD-1 and in TIG-3 cells, respectively. As shown in Fig. 1b, we selected and validated 29 of the indentified HIF-1α binding sites by real-time PCR. We confirmed that 28 cases (97%) showed at least a fourfold signal enrichment in the immunoprecipitated

**Fig. 1** Identification of HIF-1α binding sites. **a** Representative sites identified as "hypoxia-responsive", "hypoxia-enriched" and "non-hypoxia-responsive" HIF-1α binding sites. The definitions for each group are described in the text. The former two categories were considered for identifying HIF-1α target genes. *Blue* and *red* horizontal bars indicate 36-bp sequence tags that were mapped to the forward and reverse strands, respectively. The genomic coordinates and RefSeq IDs of the indicated transcript models are shown in the margin. **b** Validation of the identified binding sites by ChIP-Seq analysis using real-time PCR. The fold enrichment of the signals determined for immunoprecipitated samples compared with the background noise is shown on a log scale for 29 selected cases. Genomic regions as specified in Supplementary Table 1 were used for the validation analysis. For details, see "Materials and methods" and Supplementary Fig. 2. Error bars represent the standard deviations of triplicate experiments. (Color figure online)



**A**

**Hypoxia-responsive binding sites**

**Hypoxia-specific**

**Hypoxia-enriched**

**Non-hypoxia-responsive binding sites**

Hypoxia

Normoxia

NM_001008541 MXI1
Chr10
111,959,743 – 111,959,945

NM_184041 ALDOA
Chr10
29,984,272 – 29,948,492

Non-gene-corresponding
Chr19
6,527,869 - 6,527,993

**B**



Real time PCR enrichment (Log10(IP/WCE))

HIF-1α binding sites

samples compared with the background noise (see also Supplementary Fig. 2 for agarose gel images of the PCR bands).

Using the identified "hypoxia-responsive" HIF-1α binding sites, we searched for the HRE motif. We found that 441 (83%) and 413 (67%) regions contained the HRE motif in DLD-1 and in TIG-3 cells, respectively (fourth column, Table 1). These frequencies were similar to those reported in previous HIF-1α ChIP-chip studies (Mole et al. 2009; Xia et al. 2009), although the detected genomic regions containing the HIF-1α binding sites were shorter in length due to the improved resolution of the analysis (the lengths of the detected binding sites were more than threefold shorter than those detected in previous studies using ChIP-chip, which reflected the intervals of the designed DNA probes (Mole et al. 2009); see also Supplementary Fig. 3a). Occasionally, two or three adjacent core HRE motifs were detected in a single gene, such as the

genes encoding transferrin and the glucose transporter (Wenger et al. 2005). We examined the number of HRE motifs and the ChIP-Seq tag concentrations and found no correlation between them (Supplementary Fig. 3b). The HRE motif plays a role in defining the binding positions but may not contribute directly to the binding strength.

**Transcripts in the proximal regions of the identified HIF-1α binding sites**

In DLD-1 and TIG-3 cells, 193 (37%) and 161 (26%) of the "hypoxia-responsive" HIF-1α binding sites, respectively, were located from 10 kb upstream to 1 kb downstream of the 5′-ends of the RefSeq transcript models (23771 transcript models in 18,001 genes in total). The locations of the binding sites relative to the RefSeq genes are summarized in Venn diagrams in Fig. 2a. For these binding sites, we analyzed the distributions of the relative distances from the

**Table 1** Number of HIF-1α binding sites

| | Hypoxia-responsive binding sites | | | | Non-hypoxia-responsive binding sites |
|---|---|---|---|---|---|
| | Hypoxia-specific | Hypoxia-enriched | Total binding sites | Sites containing HRE | |
| DLD-1 | 499 | 32 | 531 | 441 (83%) | 35 |
| TIG-3 | 599 | 17 | 616 | 413 (67%) | 54 |

The number of identified HIF-1α binding sites in DLD-1 and TIG-3 cells. "Hypoxic-responsive" HIF-1α binding sites are the sum of the "hypoxia-specific" binding sites, which were detected only under hypoxia, and the "hypoxia-induced" binding sites, which were detected under normoxia, but the ChIP-Seq tag concentration was induced more than twofold under hypoxia. Note that most of the identified "hypoxia-responsive" HIF-1α binding sites are "hypoxia-specific." *HRE* hypoxia response element, 5′-RCGTG-3′
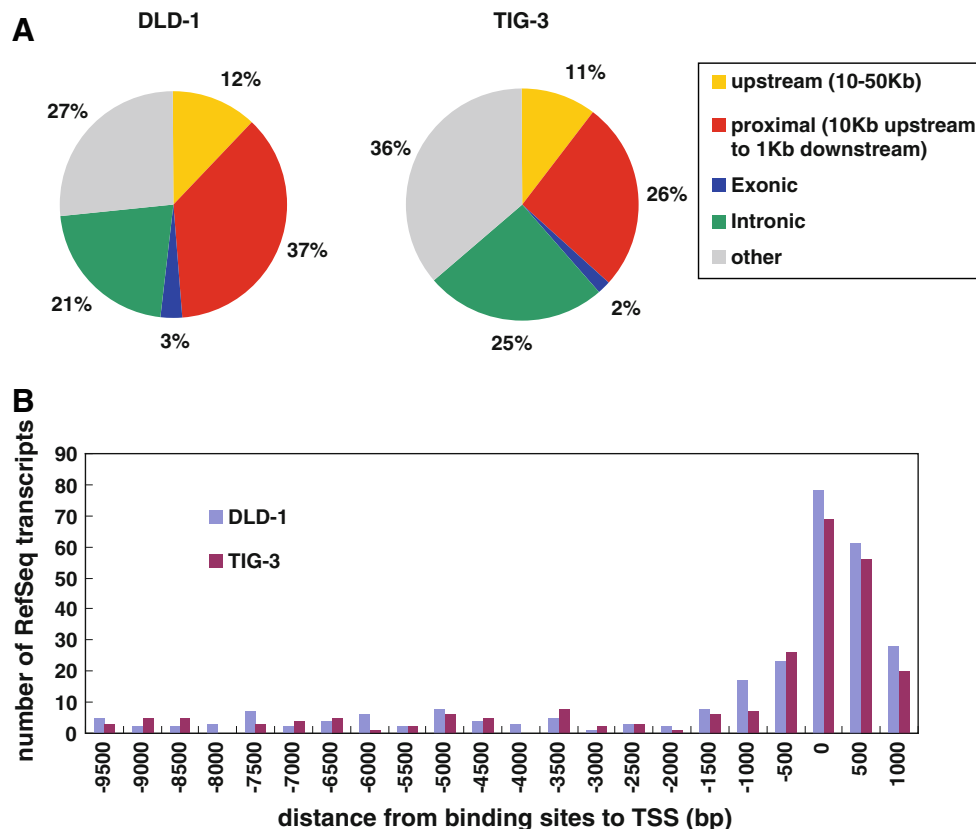


**Fig. 2** Characterization of RefSeq transcripts. **a** Genomic locations of the identified HIF-1α binding sites in DLD-1 and TIG-3 cells compared to the RefSeq transcript models. Positions relative to the RefSeq genes are shown. When a RefSeq gene contained multiple transcript models, all of the transcript models were considered.

**b** Distributions of the distances from the identified binding sites to the 5′-ends of the RefSeq transcript models. *Blue* and *red bars* represent DLD-1 and TIG-3 cells, respectively. When a RefSeq gene contained multiple transcript models, all of the transcript models were considered and counted redundantly. (Color figure online)

5′-ends of each RefSeq transcript model (Fig. 2b). When a RefSeq gene contained multiple transcript variant models, all of the variants were considered and counted redundantly. We found that approximately 70% of the binding sites were located within 1 kb of the 5′-ends of the RefSeq transcript models, which is consistent with previous estimations (Lin et al. 2009; Mole et al. 2009).

To directly examine the positions of the TSSs and their expression changes in response to HIF-1α binding in DLD-1 and TIG-3 cells, we used TSS-Seq data. This dataset contains a total of 141,590,200 TSS tags, each of which corresponds to the cap site of a single mRNA (Tsuchihara et al. 2009). We clustered the TSS tags into TSS clusters (TSCs) to separate individual putative promoter units (see the reference (Tsuchihara et al. 2009) for details). The numbers of TSS tags were normalized to parts per million mapped TSS tags, and the sum of the TSS tag concentrations associated with the same TSC was defined as the expression level of the TSC. The fold changes of each TSC in response to hypoxia were evaluated as the changes in
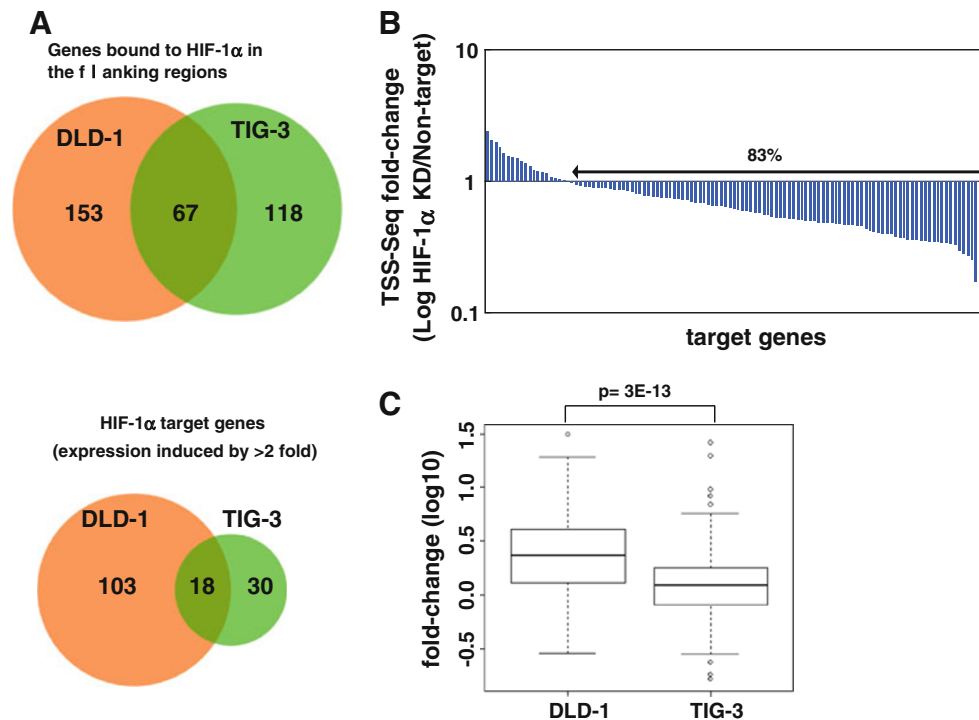
**Fig. 3** Correlations of HIF-1α target genes and their expression levels. **a** Venn diagram of the number of identified HIF-1α target genes in DLD-1 and TIG-3 cells. The *upper panel* shows the total number of genes for which HIF-1α binding sites were identified in the flanking regions. The *lower panel* shows the identified target genes with expression levels that were induced more than twofold under hypoxia, as determined on the basis of digital TSS tag counts. **b** Fold changes in the expression levels of the identified target genes in HIF-1α knock-down cells. The fold changes were calculated as the TSS tag concentration in knock-down cells/TSS tag concentration in normal cells. The *bars* below the axis represent cases in which gene expression was repressed in HIF-1α knockdown cells in comparison to normal cells (83% of all cases). See Supplementary Fig. 4 for details of the validation analysis. **c** Distributions of the fold changes in expression levels of the genes bound by HIF-1α in DLD-1 and TIG-3 cells, as determined by the digital TSS tag counts. The statistical significance of the difference in distributions was evaluated using the Wilcoxon rank sum test ($P = 1e–13$)

TSS tag concentrations under hypoxia versus normoxia. [The statistics obtained for the TSS tags are shown in Supplementary Fig. 4. Additional details can be also found in the reference (Tsuchihara et al. 2009).]

We combined the ChIP-Seq and TSS-Seq data to examine the transcriptional consequences of HIF-1α binding. Among the above-mentioned binding sites, which were associated with the RefSeq genes, the TSS-Seq data revealed the presence of TSCs that overlapped the 5'-ends of the RefSeq transcript models in 220 and 185 genes in DLD-1 and TIG-3 cells, respectively (note that a particular binding site sometimes corresponds to multiple TSCs). Particularly, in 121 and 48 genes, the expression levels of the TSCs were induced more than twofold under hypoxia, respectively, (Fig. 3a; referred to as "HIF-1α target genes/ TSCs" hereafter). As shown in Supplementary Fig. 4c, the expression levels of representative target genes were validated by real-time PCR. We also performed similar TSS-Seq analyses in HIF-1α knock-down cells. Of the 121 putative HIF-1α target genes in DLD-1 cells, the hypoxia-responsive induction of gene expression was repressed in 100 cases in the TSS-Seq analysis in which HIF-1α was knocked down (83%; Fig. 3b). Supplementary File contains the top 25 HIF-1α target genes, which are ranked according to their fold change at the transcription level in DLD-1 and TIG-3 cells (see also Supplementary Fig. 5 for an example of HIF-1α target genes identified by ChIP-Seq and TSS-Seq analyses).

We further analyzed whether the identified HIF-1α targets were translated into proteins. To achieve this goal, we analyzed the RNAs that were incorporated into the translating ribosome (polysome) fractions. RNA was isolated from DLD-1 cells that were cultured under normal and hypoxic conditions. Polysome-incorporated RNA was isolated from each cell culture by sucrose density gradient purification of the cytoplasmic RNA (see "Materials and methods"). A total of 46,170,807 36-bp single-end-read RNA-Seq tags were generated, and the abundance of the transcripts was evaluated by digital counts of the RNA-Seq tags (Supplementary Fig. 6). We expected that the changes in the RNA-Seq tags could be used as an indicator to measure gene expression changes at the translational level. As shown in Fig. 4, the levels of RNA-Seq tags for the putative HIF-1α target genes were significantly induced in

P = 3E-3

P = 2E-16
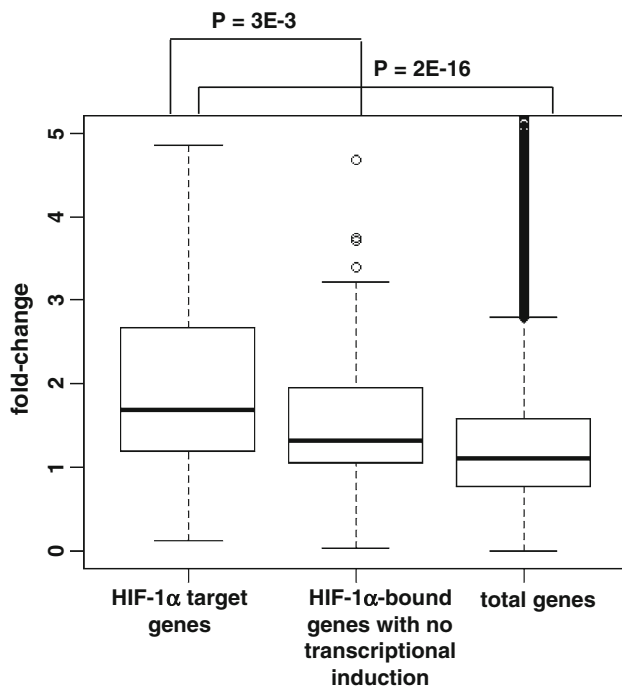


**Fig. 4** Fold change in the amount of RNA present in polysome fractions in response to hypoxic stimuli. Distributions of the fold changes of transcripts in the polysome fractions in response to hypoxia, as determined by digital RNA-Seq tag counts. Fold changes in HIF-1α-bound target genes for which transcriptional induction was observed (*left*), HIF-1α-bound genes for which no transcriptional induction was observed (*middle*) and all RefSeq genes (*right*) are shown. Statistical significance in the differences in the distributions were evaluated using the Wilcoxon rank sum test and are shown in the margin

the polysome fractions in response to hypoxia, which suggested that a majority of the gene expression was induced at the protein level, too. Taking these results together, we concluded that we had identified direct targets of HIF-1α that were bound by HIF-1α and that the expression of these targets was induced at transcriptional and translational levels.

Target genes of HIF-1α in DLD-1 and TIG-3 cells

We compared the HIF-1α target genes in DLD-1 cells and TIG-3 cells. We found that 18 genes overlapped, and the remaining genes were unique to each cell type. We performed Gene Ontology (GO) term (Ashburner et al. 2000) analysis to examine whether the gene groups of particular functional categories were enriched in the respective cell types. Seven and four GO terms were enriched (hypergeometric distribution; $P < 0.01$) in DLD-1 and TIG-3 cells, respectively (see also Supplementary Tables 2a and 2b for the full list). Of these, GO term "glycolysis" (GO: 0006096) was commonly enriched. "Response to hypoxia" (GO: 0001666) was enriched only in DLD-1 cells. It was intriguing that the genes belonging to this GO term, which

are considered to have indispensable roles in the maintenance of homeostasis under hypoxic conditions, were selectively enriched in DLD-1 cells (proportion test; $P = 0.0001$). TIG-3 cells, which represent a normal cell type and thus have never been exposed to hypoxia, may not be robust in hypoxia because several essential genes are not induced.

We also found that the hypoxic response of DLD-1 cells was more significant than that of TIG-3 cells, both in the number of target genes and in the degree of expression induced (Wilcoxon rank sum test; $P = 3e{-}13$). Figure 3c illustrates the fold expression changes in DLD-1 and TIG-3 cells.

To further characterize the molecular mechanisms underlying the differential gene expression observed between the cell types, we assessed the global expression patterns of transcription factors in DLD-1 cells and TIG-3 cells on the basis of digital TSS tag counts for the genes encoding transcription factors. We used a total of 140 well-characterized transcription factors that were registered in the representative database TRANSFAC. As shown in Supplementary Fig. 7, transcriptional induction of the transcription factor genes was more significant in DLD-1 cells than in TIG-3 cells ($P = 0.02$) (see also Supplementary Fig. 8 for an example). To specify the transcription factors that might be responsible for the activation of particular genes, we examined the enrichment of consensus binding sites for specific transcription factors in the surrounding regions of HIF-1α binding sites. We examined the genes which were identified as HIF-1α target genes in DLD-1 cells, TIG-3 cells or in both cell types. We found that fourteen consensus binding sequences were enriched around the HIF-1α binding sites in total. Of these sequences, four transcription factors were transcriptionally induced more than twofold in the TSS-Seq analysis in the corresponding cell types (see Supplementary Table 3 for the full list). These transcription factors may regulate the transcription of HIF-1α target genes in cooperation with HIF-1α in DLD-1 cells or TIG-3 cells. It is also interesting to speculate that the coordinated expression of the transcription factors might have been acquired throughout cellular history. DLD-1 cells originated from a solid tumor that experienced severe hypoxic conditions (Rajaganeshan et al. 2009; Schmitz et al. 2009). Similar analyses will be necessary in the future to assess a greater variety of cell types in order to validate this hypothesis.

Epigenetic regulation in regions surrounding HIF-1α binding sites

We also analyzed the nucleosome structure in the surrounding regions of the HIF-1α binding sites in DLD-1 and TIG-3 cells. It has been reported that nucleosomes acquire
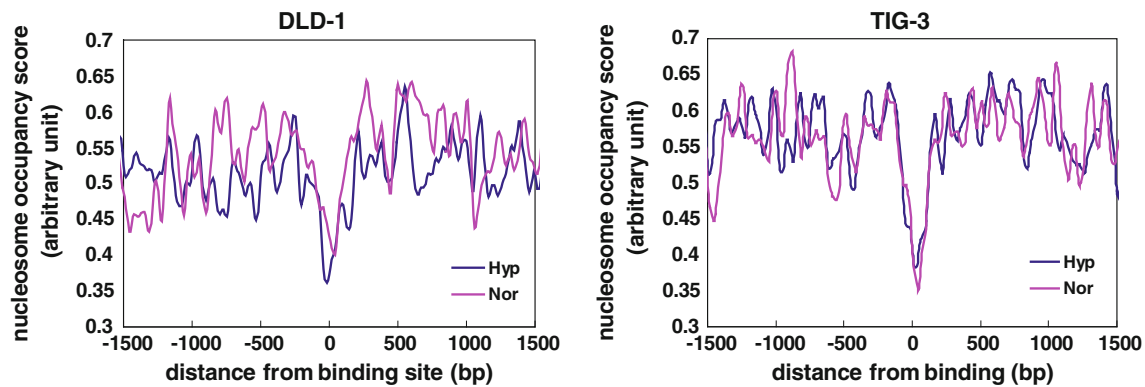
**Fig. 5** Nucleosome structures in regions surrounding HIF-1α binding sites. Nucleosome occupancy in regions surrounding the identified HIF-1α binding sites. The calculated nucleosome occupancy scores (y-axis) are plotted against every genomic coordinate (x-axis). The computational procedure used to calculate the nucleosome occupancy score is described in "Materials and methods". The putative binding site of HIF-1α, represented by HRE, was defined as position 0 (x-axis). *Blue* and *red* lines indicate the nucleosome occupancy scores under hypoxia and normoxia, respectively. Only the HIF-1α binding sites for which the associated TSCs were induced by more than twofold were used in the plot for each cell type. For details regarding the Nucleosome-Seq datasets, see Supplementary Fig. 9. (Color figure online)

an open chromatin structure following the binding of transcription factors (Zhang et al. 2009). To analyze the nucleosome structure, Nucleosome-Seq (Albert et al. 2007; Jiang and Pugh 2009; Schones et al. 2008) was used in DLD-1 and TIG-3 cells. We generated a total of 130,088,634 36-bp sequence tags from micrococcal nuclease-digested genomic DNA and calculated the occupancy of the nucleosome according to a previously reported procedure (Albert et al. 2007) (Supplementary Fig. 9; see "Materials and methods"). As shown in Fig. 5, the occupancy score for DLD-1 cells dropped sharply in the regions surrounding hypoxia-responsive HIF-1α binding sites under hypoxia (Fig. 5, blue line in the left panel), which suggested that the nucleosome structures formed an open structure. On the other hand, the occupancy scores for HRE motifs that were not bound by HIF-1α did not indicate such an open structure (Supplementary Fig. 10). The same results were obtained for TIG-3 cells (Fig. 5, blue line in the right panel). These results indicated that only a part of HRE motifs had an open nucleosome structure suitable for subsequent transcriptional activation, although HRE motifs were present throughout the human genomic sequences. Previous HIF-1α ChIP-chip studies have reported that less than 1% of the HRE motifs within the genomic sequences that are located in regions used for the microarrays are bound by HIF-1α (Mole et al. 2009; Wenger et al. 1998, 2005). Epigenetic regulation of the human genome plays an essential role in specifying the binding sites of HIF-1α in addition to the consensus binding sequences.

Interestingly, for the HIF-1α target HRE, we observed that the open chromatin structure was already formed under normoxia (Fig. 5, red line in the left panel for DLD-1 cells and in the right panel for TIG-3 cells). On the other hand,

the TSS tags induced by hypoxia for the approximately 1-kb downstream regions were first detected after the binding of HIF-1α under hypoxia. To further examine the chromatin status surrounding HIF-1α binding regions, we analyzed the histone modification patterns (H3K4me3, H3Ac and H3K27me3) and binding status of pol II by ChIP-Seq analyses. The numbers of sequence tags generated for each analysis are shown in Supplementary Fig. 11 and 12. Figure 6 shows the observed histone modification and pol II binding profiles in the regions surrounding the HIF-1α binding sites. Consistent with the TSS-Seq profiles, pol II binding first increased under hypoxia. On the other hand, the histone markers for active chromatin, H3K4me3 and H3Ac, were already observed under normoxia, whereas the marker for silent chromatin, H3K27me3, was absent throughout the hypoxic shock period (Fig. 6b–d, f–h). These results suggested that open and active chromatin structures originally formed under normoxia, irrespective of the pol II binding status and downstream transcriptional induction. The cells seemed to stay in a somewhat prepared status for a hypoxic response. The cels might memorize their histories with respect to the chromatin status. Such a prepared status of the cells via epigenetic regulation has been discussed in previous reports (Heintzman et al. 2007; Kim et al. 2008; Mole et al. 2009); however, this is the first study to provide direct evidence supporting this possibility.

### HIF-1α regulation of alternative promoter variants

One of the greatest advantages of using ChIP-Seq and TSS-Seq is that the HIF-1α binding sites and subsequent transcriptional induction can be detected separately for alternative promoters. Of the identified 121 and 48 HIF-1α
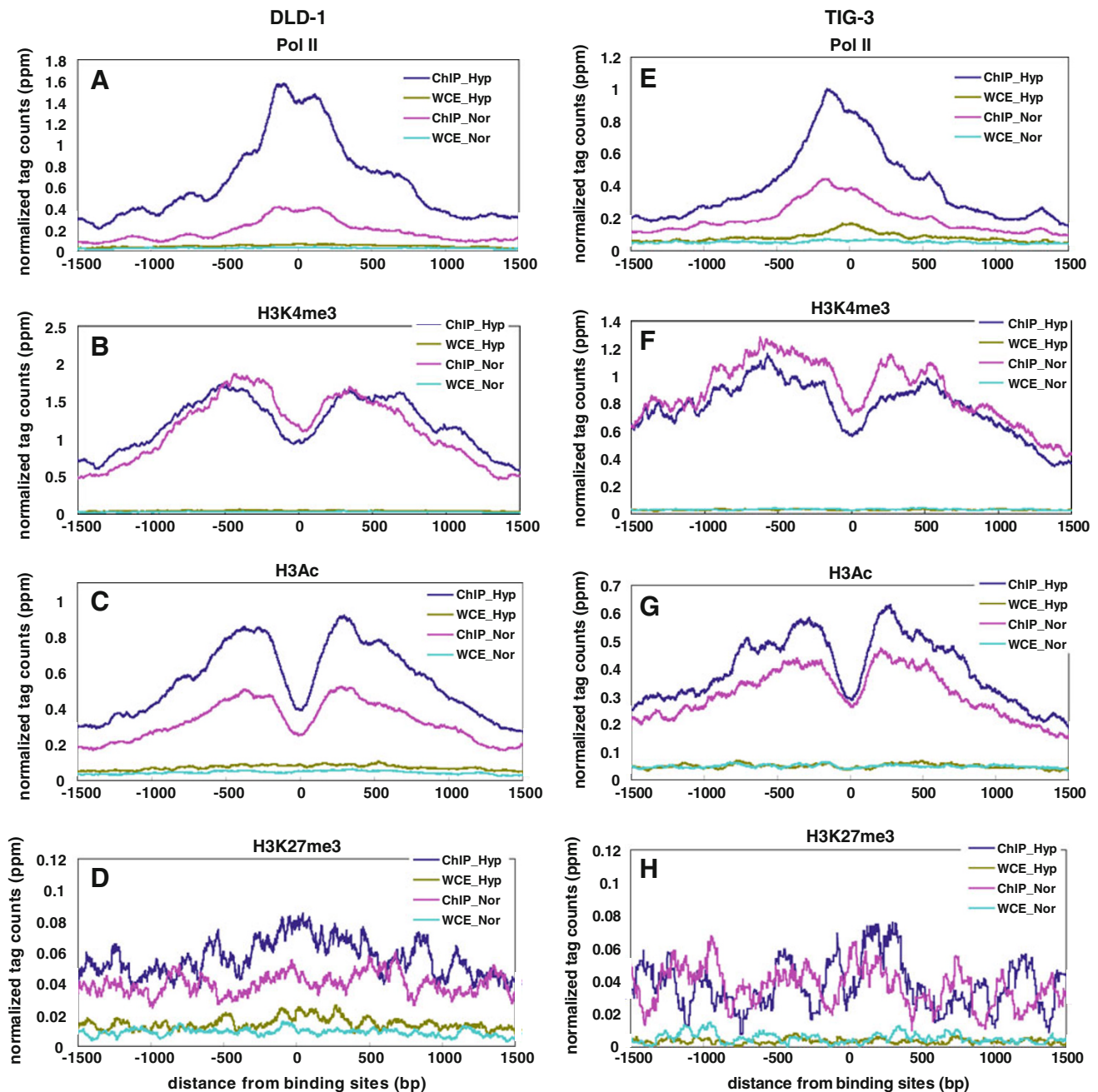
**Fig. 6** Profiles of RNA polymerase II binding and histone modification in the regions surrounding HIF-1α binding sites. Average tag concentrations (y-axis) obtained in the ChIP-Seq analyses of pol II (**a**, **e**), H3K4me3 (**b**, **f**), H3Ac (**c**, **g**) and H3K27me3 (**d**, **h**) are plotted for each genomic coordinate (x-axis). The observed profiles are shown for DLD-1 (**a–d**) and TIG-3 cells (**e–h**). In each panel, *red* and *blue lines* represent the tag counts under hypoxia and normoxia for the IP samples, respectively. *Green* and *sky blue lines* represent the results obtained for the background control (whole cell extract samples). The putative binding site of HIF-1α, represented by HRE, was defined as position 0 (x-axis). For each panel, the tag counts for 290 and 221 binding sites, which have HRE among the HIF-1α target TSCs (either geneic or intergenic TSCs), were averaged in DLD-1 and TIG-3 cells, respectively. (Color figure online)

target genes, 15 and 5 target genes had more than one alternative promoter variant in the RefSeq transcript models in DLD-1 and TIG-3 cells, respectively (see Supplementary Fig. 13 for one of these examples). It should

also be noted that the majority of HIF-1α target alternative promoters are novel promoters. One hundred and ninety-three and 123 TSCs were identified as previously uncharacterized putative alternative promoters in DLD-1 and

**Table 2** Number of TSCs associated with binding sites located in genic and intergenic regions

| | #Binding sites | #HIF-1α bound genes in which TSCs overlapped the 5′-end of RefSeq transcript models | #HIF-1α target genes |
|---|---|---|---|
| **a** | | | |
| DLD-1 | 193 | 220 | 121 |
| TIG-3 | 161 | 185 | 48 |
| | #Previously characterized AP TSCs (#genes) | | #Newly identified AP TSCs (#genes) |
| **b** | | | |
| DLD-1 | 15 (15) | | 193 (89) |
| TIG-3 | 5 (4) | | 123 (80) |
| | #Binding sites | #Intergenic TSCs | #Intergenic TSCs located in repetitive regions |
| **c** | | | |
| DLD-1 | 207 | 262 | 21 |
| TIG-3 | 289 | 105 | 21 |

**a** The number of genes that were bound to HIF-1α in the flanking regions (from 10 kb upstream to 1 kb downstream of the binding sites) of the 5′-ends in the RefSeq transcript models. "HIF-1α target genes" indicate genes with expression levels that were induced more than twofold by hypoxia

**b** The number of HIF-1α target TSCs corresponding to alternative promoters (APs) which had been characterized as RefSeq transcript variants (first column) and those which were newly identified in this study (second column). The numbers of corresponding genes are shown in parentheses

**c** The number of HIF-1α target TSCs located in intergenic regions

TIG-3 cells, respectively (Table 2b). The overlap of newly identified HIF-1α target alternative promoters with previously characterized transcript models that are present in representative databases is shown in Supplementary Table 4. It is possible there is an unexpectedly large population of the hitherto undiscovered alternative promoters involved in hypoxic response of cells.

HIF-1α binding sites in intergenic regions

The combination of ChIP-Seq and TSS-Seq allowed us to identify HIF-1α targets even in previously unannotated (so-called "intergenic") regions. Approximately one-third of the HIF-1α binding sites were located in regions that were >50 kb from the nearest RefSeq genes. For these intergenic binding sites, we searched for TSCs located from 1 kb upstream to 10 kb downstream of the HIF-1α binding sites and identified 262 and 105 putative HIF-1α target TSCs in DLD-1 and TIG-3 cells, respectively (Table 2). Twenty-one and 21 binding sites were located in repetitive regions (see also Supplementary Table 5), which suggested that some HIF-1α target sites might also have arose from repetitive regions, as previously reported for several transcription factors (Tomilin 2008; Polak and Domany 2006) (see Supplementary Fig. 14 for one of these examples). We

also found that the distributions of the distances from HIF-1α binding sites to TSCs were similar to those determined for the HIF-1α target RefSeq genes (Supplementary Fig. 15).

We searched the completely sequenced full-length cDNAs that corresponded to these TSCs and found seven overlapping cDNAs from the FLJ (Ota et al. 2004) and MGC (Gerhard et al. 2004) cDNA collections in DLD-1 and TIG-3 cells (Supplementary Table 6a). All of the corresponding full-length cDNAs lacked clear open reading frames. We determined the complete sequences of the overlapping ESTs for an additional three cases and obtained similar results (Supplementary Table 6b). An analysis of the RNA-Seq tags in the polysome fractions also suggested that majority of these intergenic HIF-1α targets were not translated (Supplementary Fig. 6c). Therefore, the intergenic TSCs of HIF-1α targets should be used to transcribe hypoxia-responsive non-protein-coding transcripts (Wilusz et al. 2009).

To determine whether these TSCs were precursors of micro-RNAs (He and Hannon 2004), we searched for miRNAs registered in the miRBase (Griffiths-Jones et al. 2006) from 10 kb upstream to 50 kb downstream of the intergenic HIF-1α binding sites. No miRNAs were located within these regions. Furthermore, we could not detect any

overlap against the previously reported repertoire of putatively-functional long non-coding RNAs (Guttman et al. 2009). We considered that these intergenic TSCs were not derived from our experimental errors, especially those identified in DLD-1 cells (Barski et al. 2007; Welboren et al. 2009), since we detected clear binding signals for pol II around 61 (21%) and 2 (2%) intergenic TSC targets of HIF-1α. These results collectively suggested that we had identified putative non-protein-coding transcript targets of HIF-1α that were comparable to the canonical RefSeq targets with respect to the number of targets and their levels of induction. However, further analyses are needed to determine the biological relevance underlying the induction of these non-coding transcripts.

## Conclusion

In the present paper, we describe the genome-wide identification of HIF-1α binding sites in the cancerous DLD-1 cell line and the normal lung fibroblast TIG-3 cell line using ChIP-Seq. We utilized several types of Illumina GA analyses to further characterize the identified binding sites. The greatest advantages of using massively parallel sequencers may be the ability to obtain versatile biological data. In fact, we were able to obtain extensive biological information that allowed us to interpret the binding events; such information could not have been obtained using ChIP-chip or microarray analysis alone. We unexpectedly discovered that HIF-1α binding sites regulate an unexpectedly large population of alternative promoters and putative non-coding transcripts. These categories of the transcripts may also contribute to hypoxic response of the cell, though they have been overlooked in previous studies. The analyses targeting these transcripts were first enabled by the single-base resolution of massively parallel sequencing technologies, for which no previous knowledge was necessary for the probe design.

An obvious limitation of the present study was the use of only two cell types. Thus, we could not identify all of the possible binding sites of HIF-1α. The identification of different targets in DLD-1 and TIG-3 cells indicates that similar analyses should be conducted using a wider variety of cell types. In addition, our stringent criteria may have precluded the identification of many genuine targets. Indeed, some genes that have been well characterized as HIF-1α target genes were not found in our study, including the telomerase (TERT) gene (Nishi et al. 2004), the vascular endothelial growth factor A (VEGFA) gene (Carmeliet et al. 1998; Forsythe et al. 1996) and the erythropoietin gene (Semenza and Wang 1992) [also note that this result is similar to that obtained in a previous ChIP-chip analysis (Mole et al. 2009)].

All of the data generated in the present study were essentially the sequence data; however, we believe that the applications of massive sequencing at various biological levels have yielded substantial biological indications. We could find that the epigenetic regulation of chromatin status and the differential repertoires of expressed transcription factors played essential roles in the cell-type-specific induction of target genes in DLD-1 and TIG-3 cells in response to hypoxia. Further extensive analyses of epigenetic changes in cancer and normal cells using Nucleosome-Seq and ChIP-Seq and of the expression patterns of transcriptions factors using TSS-Seq or RNA-Seq could reveal the mechanisms by which the differential responses of various cells to hypoxia are encoded. Such information could reveal how hypoxic cellular responses are mediated by HIF-1α in a wide variety of cancer cells.

## References

Albert I, Mavrich TN, Tomsho LP, Qi J, Zanton SJ, Schuster SC, Pugh BF (2007) Translational and rotational settings of H2A.Z nucleosomes across the *Saccharomyces cerevisiae* genome. Nature 446:572–576

Ashburner M, Ball CA, Blake JA, Botstein D, Butler H, Cherry JM, Davis AP, Dolinski K, Dwight SS, Eppig JT, Harris MA, Hill DP, Issel-Tarver L, Kasarskis A, Lewis S, Matese JC, Richardson JE, Ringwald M, Rubin GM, Sherlock G (2000) Gene ontology: tool for the unification of biology. The gene ontology consortium. Nat Genet 25(1):25

Barski A, Cuddapah S, Cui K, Roh TY, Schones DE, Wang Z, Wei G, Chepelev I, Zhao K (2007) High-resolution profiling of histone methylations in the human genome. Cell 129(4):823–837

Benita Y, Kikuchi H, Smith AD, Zhang MQ, Chung DC, Xavier RJ (2009) An integrative genomics approach identifies hypoxia inducible Factor-1 (HIF-1)-target genes that form the core response to hypoxia. Nucleic Acids Res 37(14):4587–4602

Carmeliet P, Dor Y, Herbert JM, Fukumura D, Brusselmans K, Dewerchin M, Neeman M, Bono F, Abramovitch R, Maxwell P, Koch CJ, Ratcliffe P, Moons L, Jain RK, Collen D, Keshert E (1998) Role of HIF-1alpha in hypoxia-mediated apoptosis, cell proliferation and tumour angiogenesis. Nature 394(6692):485–490

Davuluri RV, Suzuki Y, Sugano S, Plass C, Huang TH (2008) The functional consequences of alternative promoter use in mammalian genomes. Trends Genet 24(4):167–177

Forsythe JA, Jiang BH, Iyer NV, Agani F, Leung SW, Koos RD, Semenza GL (1996) Activation of vascular endothelial growth factor gene transcription by hypoxia-inducible factor 1. Mol Cell Biol 16(9):4604–4613

Fraisl P, Aragones J, Carmeliet P (2009) Inhibition of oxygen sensors as a therapeutic strategy for ischaemic and inflammatory disease. Nat Rev Drug Discov 8(2):139–152

Fyles AW, Milosevic M, Wong R, Kavanagh MC, Pintilie M, Sun A, Chapman W, Levin W, Manchul L, Keane TJ, Hill RP (1998) Oxygenation predicts radiation response and survival in patients with cervix cancer. Radiother Oncol 48(2):149–156

Gatenby RA, Gillies RJ (2004) Why do cancers have high aerobic glycolysis? Nat Rev Cancer 4(11):891–899

Gerhard DS, Wagner L, Feingold EA, Shenmen CM, Grouse LH, Schuler G, Klein SL, Old S, Rasooly R, Good P, Guyer M, Peck

AM, Derge JG, Lipman D, Collins FS, Jang W, Sherry S, Feolo M, Misquitta L, Lee E, Rotmistrovsky K, Greenhut SF, Schaefer CF, Buetow K, Bonner TI, Haussler D, Kent J, Kiekhaus M, Furey T, Brent M, Prange C, Schreiber K, Shapiro N, Bhat NK, Hopkins RF, Hsie F, Driscoll T, Soares MB, Casavant TL, Scheetz TE, Brown-stein MJ, Usdin TB, Toshiyuki S, Carninci P, Piao Y, Dudekula DB, Ko MS, Kawakami K, Suzuki Y, Sugano S, Gruber CE, Smith MR, Simmons B, Moore T, Waterman R, Johnson SL, Ruan Y, Wei CL, Mathavan S, Gunaratne PH, Wu J, Garcia AM, Hulyk SW, Fuh E, Yuan Y, Sneed A, Kowis C, Hodgson A, Muzny DM, McPherson J, Gibbs RA, Fahey J, Helton E, Ketteman M, Madan A, Rodrigues S, Sanchez A, Whiting M, Madari A, Young AC, Wetherby KD, Granite SJ, Kwong PN, Brinkley CP, Pearson RL, Bouffard GG, Blakesly RW, Green ED, Dickson MC, Rodriguez AC, Grimwood J, Schmutz J, Myers RM, Butterfield YS, Griffith M, Griffith OL, Krzywinski MI, Liao N, Morin R, Palmquist D, Petrescu AS, Skalska U, Smailus DE, Stott JM, Schnerch A, Schein JE, Jones SJ, Holt RA, Baross A, Marra MA, Clifton S, Makowski KA, Bosak S, Malek J (2004) The status, quality, and expansion of the NIH full-length cDNA project: the Mammalian Gene Collection (MGC). Genome Res 14(10B):2121–2127

Griffiths-Jones S, Grocock RJ, van Dongen S, Bateman A, Enright AJ (2006) miRBase: microRNA sequences, targets and gene nomenclature. Nucleic Acids Res 34(Database issue):D140–D144

Guttman M, Amit I, Garber M, French C, Lin MF, Feldser D, Huarte M, Zuk O, Carey BW, Cassady JP, Cabili MN, Jaenisch R, Mikkelsen TS, Jacks T, Hacohen N, Bernstein BE, Kellis M, Regev A, Rinn JL, Lander ES (2009) Chromatin signature reveals over a thousand highly conserved large non-coding RNAs in mammals. Nature 458(7235):223–227

Harris AL (2002) Hypoxia—a key regulatory factor in tumour growth. Nat Rev Cancer 2(1):38–47

He L, Hannon GJ (2004) MicroRNAs: small RNAs with a big role in gene regulation. Nat Rev Genet 5(7):522–531

Heintzman ND, Stuart RK, Hon G, Fu Y, Ching CW, Hawkins RD, Barrera LO, Van Calcar S, Qu C, Ching KA, Wang W, Weng Z, Green RD, Crawford GE, Ren B (2007) Distinct and predictive chromatin signatures of transcriptional promoters and enhancers in the human genome. Nat Genet 39(3):311–318

Hirota K, Semenza GL (2006) Regulation of angiogenesis by hypoxia-inducible factor 1. Crit Rev Oncol Hematol 59(1):15–26

Jiang C, Pugh BF (2009) Nucleosome positioning and gene regulation: advances through genomics. Nat Rev Genet 10(3):161–172

Keith B, Simon MC (2007) Hypoxia-inducible factors, stem cells, and cancer. Cell 129(3):465–472

Kim J, Chu J, Shen X, Wang J, Orkin SH (2008) An extended transcriptional network for pluripotency of embryonic stem cells. Cell 132(6):1049–1061

Koritzinsky M, Wouters BG (2007) Hypoxia and regulation of messenger RNA translation. Methods Enzymol 435:247–273

Kwon H, Thierry-Mieg D, Thierry-Mieg J, Kim HP, Oh J, Tunyaplin C, Carotta S, Donovan CE, Goldman ML, Tailor P, Ozato K, Levy DE, Nutt SL, Calame K, Leonard WJ (2009) Analysis of interleukin-21-induced Prdm1 gene regulation reveals functional cooperation of STAT3 and IRF4 transcription factors. Immunity 31(6):941–952

Landry JR, Mager DL, Wilhelm BT (2003) Complex controls: the role of alternative promoters in mammalian genomes. Trends Genet 19(11):640–648

Lin B, Wang J, Hong X, Yan X, Hwang D, Cho JH, Yi D, Utleg AG, Fang X, Schones DE, Zhao K, Omenn GS, Hood L (2009) Integrated expression profiling and ChIP-seq analyses of the growth inhibition response program of the androgen receptor. PLoS One 4(8):e6589

Maxwell PH (2005) The HIF pathway in cancer. Semin Cell Dev Biol 16(4–5):523–530

Mole DR, Blancher C, Copley RR, Pollard PJ, Gleadle JM, Ragoussis J, Ratcliffe PJ (2009) Genome-wide association of hypoxia-inducible factor (HIF)-1alpha and HIF-2alpha DNA binding with expression profiling of hypoxia-inducible transcripts. J Biol Chem 284(25):16767–16775

Nishi H, Nakada T, Kyo S, Inoue M, Shay JW, Isaka K (2004) Hypoxia-inducible factor 1 mediates upregulation of telomerase (hTERT). Mol Cell Biol 24(13):6076–6083

Nordsmark M, Overgaard M, Overgaard J (1996) Pretreatment oxygenation predicts radiation response in advanced squamous cell carcinoma of the head and neck. Radiother Oncol 41(1):31–39

Ortiz-Barahona A, Villar D, Pescador N, Amigo J, del Peso L (2010) Genome-wide identification of hypoxia-inducible factor binding sites and target genes by a probabilistic model integrating transcription-profiling data and in silico binding site prediction. Nucleic Acids Res 38(7):2332–2345

Ota T, Suzuki Y, Nishikawa T, Otsuki T, Sugiyama T, Irie R, Wakamatsu A, Hayashi K, Sato H, Nagai K, Kimura K, Makita H, Sekine M, Obayashi M, Nishi T, Shibahara T, Tanaka T, Ishii S, Yamamoto J, Saito K, Kawai Y, Isono Y, Nakamura Y, Nagahari K, Murakami K, Yasuda T, Iwayanagi T, Wagatsuma M, Shiratori A, Sudo H, Hosoiri T, Kaku Y, Kodaira H, Kondo H, Sugawara M, Takahashi M, Kanda K, Yokoi T, Furuya T, Kikkawa E, Omura Y, Abe K, Kamihara K, Katsuta N, Sato K, Tanikawa M, Yamazaki M, Ninomiya K, Ishibashi T, Yamashita H, Murakawa K, Fujimori K, Tanai H, Kimata M, Watanabe M, Hiraoka S, Chiba Y, Ishida S, Ono Y, Takiguchi S, Watanabe S, Yosida M, Hotuta T, Kusano J, Kanehori K, Takahashi-Fujii A, Hara H, Tanase TO, Nomura Y, Togiya S, Komai F, Hara R, Takeuchi K, Arita M, Imose N, Musashino K, Yuuki H, Oshima A, Sasaki N, Aotsuka S, Yoshikawa Y, Matsunawa H, Ichihara T, Shiohata N, Sano S, Moriya S, Momiyama H, Satoh N, Takami S, Terashima Y, Suzuki O, Nakagawa S, Senoh A, Mizoguchi H, Goto Y, Shimizu F, Wakebe H, Hishigaki H, Watanabe T, Sugiyama A, Takemoto M, Kawakami B, Yamazaki M, Watanabe K, Kumagai A, Itakura S, Fukuzumi Y, Fujimori Y, Komiyama M, Tashiro H, Tanigami A, Fujiwara T, Ono T, Yamada K, Fujii Y, Ozaki K, Hirao M, Ohmori Y, Kawabata A, Hikiji T, Kobatake N, Inagaki H, Ikema Y, Okamoto S, Okitani R, Kawakami T, Noguchi S, Itoh T, Shigeta K, Senba T, Matsumura K, Nakajima Y, Mizuno T, Morinaga M, Sasaki M, Togashi T, Oyama M, Hata H, Watanabe M, Komatsu T, Mizushima-Sugano J, Satoh T, Shirai Y, Takahashi Y, Nakagawa K, Okumura K, Nagase T, Nomura N, Kikuchi H, Masuho Y, Yamashita R, Nakai K, Yada T, Nakamura Y, Ohara O, Isogai T, Sugano S (2004) Complete sequencing and characterization of 21,243 full-length human cDNAs. Nat Genet 36(1):40–45

Park PJ (2009) ChIP-seq: advantages and challenges of a maturing technology. Nat Rev Genet 10(10):669–680

Polak P, Domany E (2006) Alu elements contain many binding sites for transcription factors and may play a role in regulation of developmental processes. BMC Genomics 7:133

Poon E, Harris AL, Ashcroft M (2009) Targeting the hypoxia-inducible factor (HIF) pathway in cancer. Expert Rev Mol Med 11:e26

Pouyssegur J, Dayan F, Mazure NM (2006) Hypoxia signalling in cancer and approaches to enforce tumour regression. Nature 441(7092):437–443

Rajaganeshan R, Prasad R, Guillou PJ, Scott N, Poston G, Jayne DG (2009) Expression patterns of hypoxic markers at the invasive margin of colorectal cancers and liver metastases. Eur J Surg Oncol 35(12):1286–1294

Raval RR, Lau KW, Tran MG, Sowter HM, Mandriota SJ, Li JL, Pugh CW, Maxwell PH, Harris AL, Ratcliffe PJ (2005) Contrasting properties of hypoxia-inducible factor 1 (HIF-1) and HIF-2 in von Hippel-Lindau-associated renal cell carcinoma. Mol Cell Biol 25(13):5675–5686

Robertson G, Hirst M, Bainbridge M, Bilenky M, Zhao Y, Zeng T, Euskirchen G, Bernier B, Varhol R, Delaney A, Thiessen N, Griffith OL, He A, Marra M, Snyder M, Jones S (2007) Genome-wide profiles of STAT1 DNA association using chromatin immunoprecipitation and massively parallel sequencing. Nat Methods 4(8):651–657

Schmitz KJ, Muller CI, Reis H, Alakus H, Winde G, Baba HA, Wohlschlaeger J, Jasani B, Fandrey J, Schmid KW (2009) Combined analysis of hypoxia-inducible factor 1 alpha and metallothionein indicates an aggressive subtype of colorectal carcinoma. Int J Colorectal Dis 24(11):1287–1296

Schones DE, Cui K, Cuddapah S, Roh TY, Barski A, Wang Z, Wei G, Zhao K (2008) Dynamic regulation of nucleosome positioning in the human genome. Cell 132(5):887–898

Semenza GL (2000) HIF-1 and human disease: one highly involved factor. Genes Dev 14(16):1983–1991

Semenza GL (2003) Targeting HIF-1 for cancer therapy. Nat Rev Cancer 3(10):721–732

Semenza GL (2010) Defining the role of hypoxia-inducible factor 1 in cancer biology and therapeutics. Oncogene 29(5):625–634

Semenza GL, Wang GL (1992) A nuclear factor induced by hypoxia via de novo protein synthesis binds to the human erythropoietin gene enhancer at a site required for transcriptional activation. Mol Cell Biol 12(12):5447–5454

Thomas JD, Johannes GJ (2007) Identification of mRNAs that continue to associate with polysomes during hypoxia. Rna 13(7):1116–1131

Tian H, McKnight SL, Russell DW (1997) Endothelial PAS domain protein 1 (EPAS1), a transcription factor selectively expressed in endothelial cells. Genes Dev 11(1):72–82

Tomilin NV (2008) Regulation of mammalian gene expression by retroelements and non-coding tandem repeats. Bioessays 30(4):338–348

Tsuchihara K, Suzuki Y, Wakaguri H, Irie T, Tanimoto K, Hashimoto S, Matsushima K, Mizushima-Sugano J, Yamashita R, Nakai K, Bentley D, Esumi H, Sugano S (2009) Massive transcriptional start site analysis of human genes in hypoxia cells. Nucleic Acids Res 37(7):2249–2263

Valouev A, Johnson DS, Sundquist A, Medina C, Anton E, Batzoglou S, Myers RM, Sidow A (2008) Genome-wide analysis of transcription factor binding sites based on ChIP-Seq data. Nat Methods 5(9):829–834

Wang GL, Semenza GL (1995) Purification and characterization of hypoxia-inducible factor 1. J Biol Chem 270(3):1230–1237

Welboren WJ, van Driel MA, Janssen-Megens EM, van Heeringen SJ, Sweep FC, Span PN, Stunnenberg HG (2009) ChIP-Seq of ERalpha and RNA polymerase II defines genes differentially responding to ligands. EMBO J 28(10):1418–1428

Wenger RH, Kvietikova I, Rolfs A, Camenisch G, Gassmann M (1998) Oxygen-regulated erythropoietin gene expression is dependent on a CpG methylation-free hypoxia-inducible factor-1 DNA-binding site. Eur J Biochem 253(3):771–777

Wenger RH, Stiehl DP, Camenisch G (2005) Integration of oxygen signaling at the consensus HRE. Sci STKE (306):re12

Wiesener MS, Jurgensen JS, Rosenberger C, Scholze CK, Horstrup JH, Warnecke C, Mandriota S, Bechmann I, Frei UA, Pugh CW, Ratcliffe PJ, Bachmann S, Maxwell PH, Eckardt KU (2003) Widespread hypoxia-inducible expression of HIF-2alpha in distinct cell populations of different organs. Faseb J 17(2):271–273

Wilusz JE, Sunwoo H, Spector DL (2009) Long noncoding RNAs: functional surprises from the RNA world. Genes Dev 23(13):1494–1504

Xia X, Kung AL (2009) Preferential binding of HIF-1 to transcriptionally active loci determines cell-type specific response to hypoxia. Genome Biol 10(10):R113

Xia X, Lemieux ME, Li W, Carroll JS, Brown M, Liu XS, Kung AL (2009) Integrative analysis of HIF binding and transactivation reveals its role in maintaining histone methylation homeostasis. Proc Natl Acad Sci U S A 106(11):4260–4265

Zhang Y, Moqtaderi Z, Rattner BP, Euskirchen G, Snyder M, Kadonaga JT, Liu XS, Struhl K (2009) Intrinsic histone-DNA interactions are not the major determinant of nucleosome positions in vivo. Nat Struct Mol Biol 16(8):847–852